Design and Evaluation of Skating Motions for a Dexterous Quadruped

Guillaume Bellegarda, Kees van Teeffelen, and Katie Byl

***Abstract*— This paper describes skating locomotion for a quadruped robot with dexterous limbs. The emphasis is on design of omnidirectional motion primitives and quantification of resulting speed and accuracy when traversing different types of smooth but potentially non-flat terrain. In particular, we study trade-offs between using four-wheeled versus three-wheeled skating maneuvers. In four-wheeled skating, motions have the benefit of symmetry, so that errors due to wheel slip should theoretically cancel out on average. Three-wheeled skating, by contrast, introduces significantly more asymmetry in configuration and contact force distribution over time; however, it has the advantage of guaranteeing continuous ground contact for all skates when terrain has bumps or other curvature. We present simulation results quantifying errors for each approach, for various terrains. Our results allow us to tune motions to reduce biases and variability in motion, which are primarily due to accelerations as locomotion begins.**

I. Introduction

While previous work has been done to develop robots that skate, it has largely focused on new robot design and/or relatively simple, symmetric motions. In this paper, we explore more diverse, omnidirectional motions for skating, to enable dual-locomotion strategies, rolling rapidly on relatively simple terrain and switching to quadruped walking for rough or intermittent terrain. Emphasis is deliberately on design parameterization and data-based evaluation, and not on presentation nor verification of approximate dynamic models, with the purposes of examining uncertainty propagation and enabling later algorithms (i.e., learning) for parameter tuning and optimization.

We study skating motions specifically designed for JPL's Robosimian quadruped [1]–[5], which is shown in Figure 1. Robosimian is designed with four identical limbs, each with seven degrees of freedom. By mounting a single-wheel skate at each forearm, six actuated degrees of freedom (DOFs) are available to set the 6-DOF pose of each skate, without interfering with the tip of the limb, which is to be used in walking gaits. While force and torque sensing are available at this most distal tip of each limb, there is currently no sensing available to sense contact of the skate with the ground. This eliminates the practical use of force feedback during skating, and as such, we focus on execution of "open-loop" motion primitives, in which encoder feedback is available and used to control desired joint angle trajectories, while the joint trajectories themselves are not updated or modified during execution based on feedback. This opens the question of what planned trajectory length is suitable, to balance the reduced cost of replanning against the increasing variability in end state as such motion sequences become longer.

Fig. 1. Versatile Locomotion with Robosimian. At top: Robosimian skating on flat ground. Bottom: Close-up of leg in quadruped modality, with skate mounted, and Robosimian bipedal and grasping a handhold during "egress of car" task at the DARPA Robotics Challenge in 2015.

There are already a wide variety of skating robots that have been studied. Among quadrupeds, perhaps the most famous skating robot is the roller-walker, which was developed and studied by Hirose and his research group [6]–[10]. The roller-walker has a reconfigurable end effector, which can be used as either a foot or skate, quite similar conceptually to the addition of a wheel we employ with Robosimian, as depicted in the lower left of Figure 1. A body of work exists on system design and motion planning for the roller-walker, for four-wheeled skating locomotion in a mostly-forward direction on flat ground. The leg-wheel concept has been extended to develop robot designs to minimize the number of required actuators, for example a unique design using a hexagonal frame [11].

This work was funded in part by NSF NRI award 1526424 and the U.S. Armys Robotics CTA through grant No. W911NF-08-R-0012.

[1]Guillaume Bellegarda and Katie Byl are with the Robotics Laboratory, Dept. of Electrical and Computer Engineering, University of California at Santa Barbara (UCSB). gbellegarda@umail.ucsb.edu, k.j.vanteeffelen@student.utwente.nl, katiebyl@ucsb.edu

Biped skating on passive wheels has also been explored by many researchers [12]–[15]. For such humanoid systems, balance becomes a greater concern, although few works deal directly with dynamic motions and generally employ static stability, using both skates always in contact. An exception includes [13], which includes two-wheel balance on a single skate, essentially becoming a special type of planar inverted pendulum system.

In this paper, we focus on skating with higher-dimensional limbs, in which all six degrees of freedom of each wheel can be controlled, with the motivation of enabling a wide range of motion primitives, ideally including agile and dynamic maneuvers. As such, it is worth briefly citing Boston Dynamics' wheeled robot Handle [16]. Although Handle uses powered wheels, rather than passive ones as in this work, the robot and its control algorithms are designed with speed and agility in mind, for sufficiently smooth terrain.

Another objective we have is to explore design and resulting performance of motion primitives for mildly stochastic terrain. Speed and accuracy of locomotion are our primary concerns. Friction variations, non-zero slopes, and bumps along terrain all clearly affect skating locomotion, and we quantify some of these effects. We hypothesize that using three wheels instead of four may increase accuracy, since wheels will stay in contact across mild terrain curvatures. However, such motions may also introduce additional asymmetries and/or uncertainties in contact forces that may not produce a net benefit in performance, motivating this study.

The rest of this paper is organized as follows. Section II describes our modeling framework for planning skate motions and subsequent joint trajectories of the robot. Section III outlines the design of simple, forward-facing motion primitives to skate in a straight line, studying both pairwise skating with all four limbs and three-wheeled skating for more consistent ground contact at all skates. Section IV presents design and results for speed and accuracy of more complex motions primitives and stochastic terrain situations, based on Monte Carlo simulations on stochastically generated terrain using Klampt (Kris' Locomotion and Manipulation Planning Toolbox) [17]. Finally, conclusions and discussion of applications toward both high-level motion planning and low-level learning for our work are presented in Section V.

II. Modeling

Planning effective, feasible skating motions for RoboSimian involves two complementary problems. The motions of the skates must enable generation of required ground reaction forces without excessive slipping, to move the robot as desired, and solutions for inverse kinematics must be tractable, smooth, and within the dynamic velocity and acceleration limits of the joint actuators of the robot.

A. Skating Kinematics and Dynamics

Each "skate" we use for RoboSimian is a simple wheel. Motions are planned assuming standard constraints for an ideal wheel. For our planning, we assume that no slip occurs

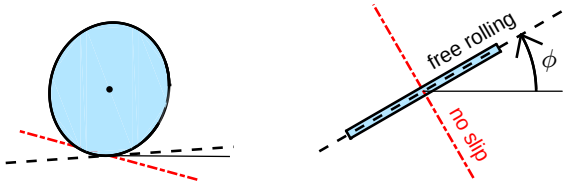

Fig. 2. Simple wheel, with constraint axes: angled and overhead views.

along the axis of the wheel, and that the wheel can roll freely perpendicular to the no-slip axis and can rotate freely about a point contact with the ground. In the no-slip direction, however, achievable lateral forces are limited by friction, so that in reality, $|F_x| \leq \mu F_z$, where μ is the coefficient of friction between the ground and the wheel, and F_z is the normal force at the ground contact. Figure 2 illustrates the no-slip and free-wheeling directions; free rotation about the contact point corresponds to angle ϕ. We also assume no force or torque can occur along the freely-moving DOFs.

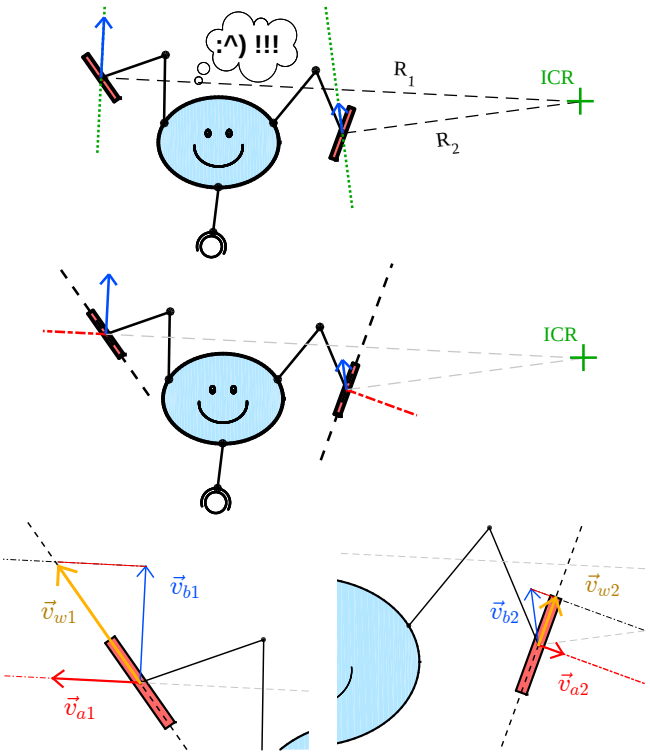

Fig. 3. Overview of planning for skating kinematics.

Given these constraints, one can plan co-compatible motions for the body (globally) and for the skates (with respect to the local body coordinate frame). As with many locomotion problems, planning can be achieved by first reasoning about allowable combinations of body and end effector motions that satisfy the required constraints. Then, enforcing those particular motions must result in the desired forces, at least to the extent that modeling assumptions for the dynamics are correct. Zero-moment point (ZMP) planning is a classic example of this basic approach, in which desired forces are achieved not directly through force feedback but

indirectly, through enforcing joint-level trajectories compatible with desired ground reaction forces [18], [19].

In Figure 3, the top image shows an overhead view of a particular pose and robot configuration. This robot example has two skates and a third spherical wheel (with no constraints on direction of free rolling), for simplicity. A desired instantaneous center of rotation (ICR) is defined for the robot body path. The ICR in turns defines the relative direction and magnitude of any point in the local body reference frame: direction will be perpendicular to the radial line, R_n, from the ICR to that point, and magnitude must be proportional to this distance. At the midpoint of each skate, the total velocity will be the sum of this local "body velocity", shown as blue vectors in this figure, plus the relative velocity of the skate with respect to the local body reference frame.

Let us also assume that we pick a particular direction of motion for each skate, depicted by the red dashed lines in the middle image. Referring to the lower left image of Fig. 3, in order for both the simple kinematic constraints shown in Figure 2 and desired absolute body trajectory motions to be achieved, the sum of the velocity due to body motion (blue vector) plus the relative velocity of skate with respect to body (red vector) must align along the "free rolling" direction of the skate (yellow vector), since no motion (i.e., slip) is assumed in the direction perpendicular to this.

During execution of the resulting motion plan, forces are generated only along the no slip axis, with zero force along the free rolling direction. So long as friction limits along the no slip axis are not exceeded, the planned constraints should theoretically be obeyed, resulting in desired body motion.

Of course, real-world skates do not have point contacts, friction on terrain is not always well-characterized or consistent, and even guarantees of expected z-directed contact forces, F_z, required for corresponding lateral friction forces, cannot necessarily be made for quadruped skating, once terrain become uneven. Coping with such non-ideal situations is a large focus of this paper.

B. Constraints Particular to RoboSimian

As mentioned in the Introduction, we mount a single wheel on the most distal link, or "forearm", of the robot. Along each limb, there are six actuated joints, more proximal to the body, which set the six degree-of-freedom (DOF) pose, i.e., location and orientation (x, y, z, roll, pitch, and yaw), of each skate. A seventh motor is located at the very end of each leg, as depicted in the lower right portion of Figure 1.

Two issues make motion planning for Robosimian particularly challenging. First, the inverse kinematics (IK) to set the 6-DOF pose of the skate require choosing from among one of eight IK families, each analogous to a choice of "elbow bending direction" for each of three elbows on a limb [3]. Providing guarantees of smoothness requires precalculation of IK solutions across a region and requires compromises between ideal theoretical contact locations and achievable solutions for our particular robot. In particular, achieving exact symmetry in end effector locations is either non-trivial or not achievable, for many desired skate configurations.

A second constraint in planning is a lack of force sensing, to detect contact and loading of the skate on the ground, as discussed in the paragraph just preceding Fig. 1. More specifically, six-DOF force and torque sensing is available at the most distal "foot" contact of each limb, but not for the attached skate for the real robot. Our simulations in Klampt obviously provide such contact force data, but we use this only in post-processing, to identify and quantify slip.

III. Design of Simple Skating Motions

This section describes three-wheeled and four-wheeled skating along a straight, forward-facing path. Note throughout that skates are numbered 1 through 4, with limb/skate 1 at the front right of the robot, and numbering continuing sequentially going clockwise when viewing the robot from above. For example, Figure 4 shows Robosimian facing to the left, within Klampt. At right, the skate in midair is on limb 4. The position of each skate (x_{ee}, y_{ee}) is measured with respect to the body frame rather than the world frame.

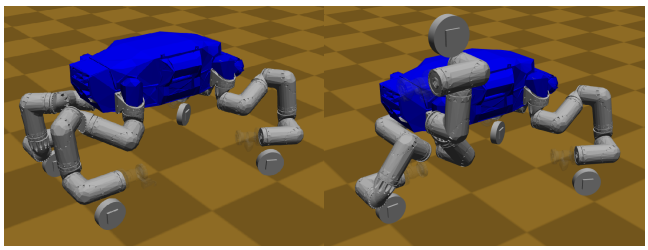

Fig. 4. RoboSimian on 4 (left) and 3 skates (right), simulated in Klampt.

For all trajectories presented in this paper, acceleration and deceleration of planned body motions follow triangular waveforms. Figure 5 illustrates this.

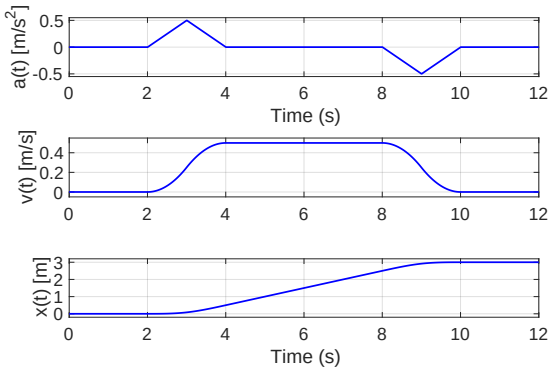

Fig. 5. Acceleration ($a(t)$), velocity ($v(t)$), and position ($x(t)$) profiles for planned robot body motions.

A. Skating with Four Wheels

Skating with four limbs/wheels exploits symmetry, canceling out some effects of slip. For straight-line body trajectories, the left versus right limbs move symmetrically with respect to one another, so that limbs 1 and 4 (front two limbs) have a phase difference of π with respect to one other (as do limbs 2 and 3). There is a phase difference of $\pi/2$

between the front and rear limbs, so that one set of skates will have maximum angle of attack, ϕ, and (correspondingly) maximum force generation potential, exactly when the other pair is aligned with the free-rolling axis pointing forward, with no ability to generate a net ground reaction force in this forward direction. This effect is especially important during acceleration and deceleration of the robot.

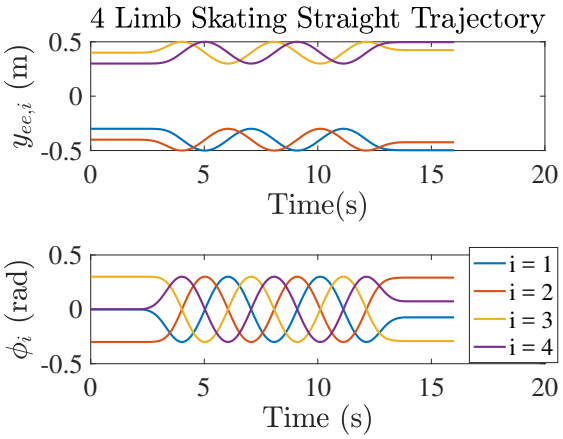

Fig. 6. Local skate end effector positions and angles ϕ for a simple, straight body trajectory with 4 skates. The front two skates are out of phase by $\pi/2$ with the back skates, and due to symmetry, are out of phase by π with each other to ensure minimal slip and maximum propulsion forces.

Figure 6 shows $y_{ee}(t)$ and $\phi(t)$ trajectories for a desired robot body motion going straight ahead, in the (forward-facing) local $+x$ direction. Each skate does not move in the x direction, with respect to the robot body frame, as the relative skate motions are perpendicular to the robot's direction of motion.

B. Skating with Three Wheels

Using only three wheels to skate has two motivations. It leaves the fourth limb free for manipulation tasks, and – more importantly – three skates provide more reliable ground contact on curved terrain profiles than four.

In planning, we assume that limb 4 (front left limb) is up and "out of the way" of any skating motions of the remaining three limbs, and primarily plan for trajectories with limb 1 placed nearly front and center of RoboSimian, as shown in Figure 4. We also designed and tested other three-skate configurations, which require additional planning and offsets, but focus on this quasi-symmetric case, which improves performance.

The basic idea in three-skate planning is to use equal phase increments between skates (i.e., "three-phase" waveforms). The asymmetry of using three skates has a significant drawback, however: it increases vulnerability to yaw due to slip during accelerations of the body. Toward mitigating this problem, we study three approaches, described below.

1) More carefully choosing the phase offset of each skate: We start with initial phase offsets of 0 for skate 1, $2\pi/3$ for skate 2, and $4\pi/3$ for skate 3. Corresponding simulations in Klampt show significant slip during the initial acceleration phase of the skating motion, causing unwanted yaw (to the left) in the actual body trajectory. Most of this yaw is due to wheel slip at skate 2 (i.e., right rear wheel).

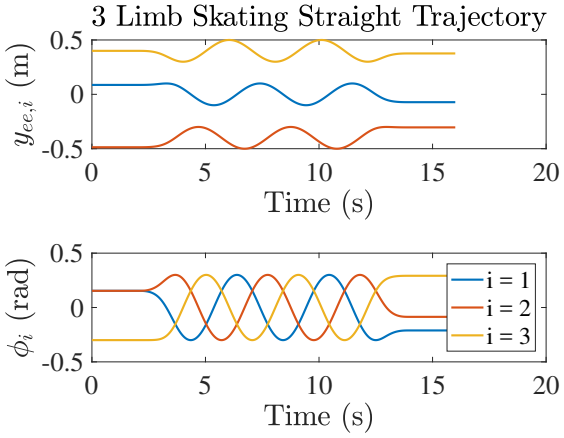

Fig. 7. Local skate end effector positions and angles ϕ for a simple, straight body trajectory with 3 skates. Each skate is out of phase by $2\pi/3$ to ensure the robot goes in a straight line, with this configuration being the optimal for straight ahead acceleration from stand still, as determined from simulations (to be later discussed) associated with Figures 8 and 9.

We study the effects of changing the phase offset at start-up by performing simulations of a 10-meter straight trajectory on a terrain with $\mu = 0.3$. Phase offsets are parameterized as $(0+\gamma, 2\pi/3+\gamma, 4\pi/3+\gamma)$ for skates 1, 2, 3, respectively, with γ set to one particular value on each trial. Resulting body coordinate trajectories are shown in Figure 8. The top plot shows the (x, y) body trajectory, while the lower plot shows yaw angle over time.

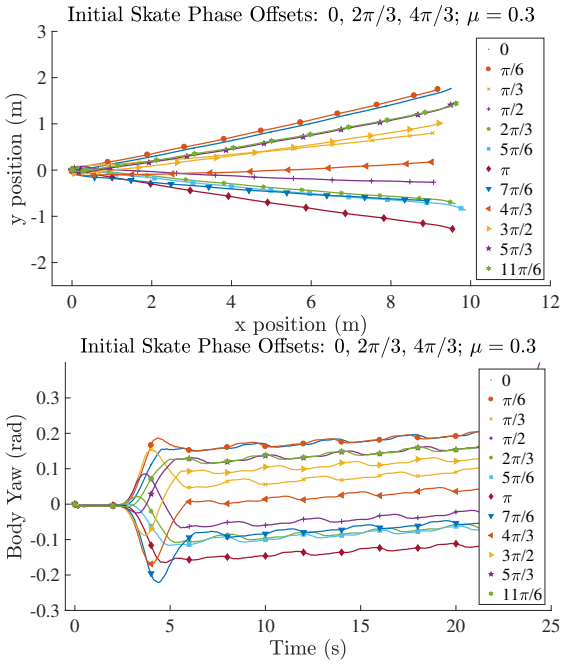

Fig. 8. Results for a 10 (m) straight trajectory, designed for 3-wheel skating, with peak of $a(t) = 0.5$ (m/s^2) at the midpoint of a 2-second triangular acceleration profile, reaching a steady-state velocity of 0.5 (m/s), with a deceleration over the last 2 seconds of the trajectory. The phase offset, γ, is changed incrementally by $\pi/6$.

Figure 9 shows results for a similar case, except reversing the sign on the 120° phase offsets among skates, to use offsets of $(0+\gamma, 4\pi/3+\gamma, 2\pi/3+\gamma)$.

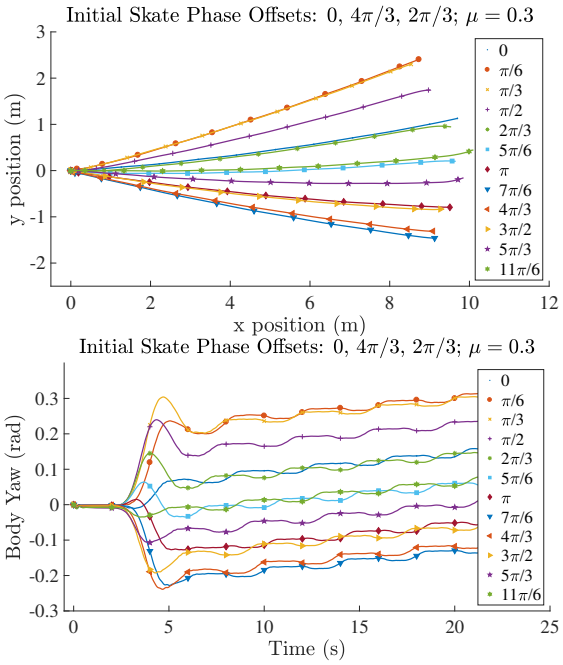

Fig. 9. Using the same body trajectory as in Fig. 8 and again changing the phase offset for each skate incrementally by $\pi/6$, but with the reversed order of phase increment among the three skates.

The two choices of symmetric phase offset for three-wheel skating should produce identical steady-state motions, in theory. In simulation, however, each has different (non-ideal) "problems", due to asymmetries now. For Fig. 8, using $(\gamma, \gamma+120°, \gamma+240°)$, the straightest trajectory is for $\gamma = 4\pi/3$; however, total distance traveled (upper subplot) has a 10% error, going only about 9 meters, instead of 10. For a reversed skate phasing of $(\gamma, \gamma-120°, \gamma-240°)$, Fig. 9 shows a somewhat more significant steady-state rate of undesired body yaw (turning to the left, for each case), but this rate is quite small in both cases, i.e., 0.17 $(°/s)$ vs 0.30 $(°/s)$, which map to circular paths with radii of 170 vs 95 meters (i.e., very slight turning, indeed).

More importantly, the steady-state velocity for the latter case is now much closer to its planned value. With $\gamma = 11\pi/6$, total distance traveled is almost exactly the desired distance of 10 m, as shown on the top subplot of Fig. 9, versus the 10% error mentioned above for Fig. 8.

For the remaining three-skate trajectories presented in this paper, an initial configuration of $(0, 4\pi/3, 2\pi/3) + 11\pi/6$ is used as an "optimal offset", since it minimizes error in Figure 9. Fig. 7 in fact presents ϕ and y for this particular parameterization. Note that during acceleration (near $t = 4$ s), the front skate ($i = 1$) is the one pointing most nearly "straight forward", while the two back wheels, though still asymmetric with respect to one another, push in opposite directions, for an effect that somewhat mimics the symmetry of four limb skating.

2) Slowing down the initial acceleration rate from a stand still: We compared simulation results for both the initial acceleration profile shown in Fig. 5 and for a similar profile that instead uses half the peak acceleration, spread over twice the time (four seconds instead of two), to reach the same steady-state velocity of 0.5 (m/s), to compare errors in body trajectory during acceleration. The slower acceleration reduces required lateral forces (reducing chance of slip) but also clearly increases required time to go a particular distance, so that we anticipate a classic trade-off between speed and accuracy, in tracking planned body motions.

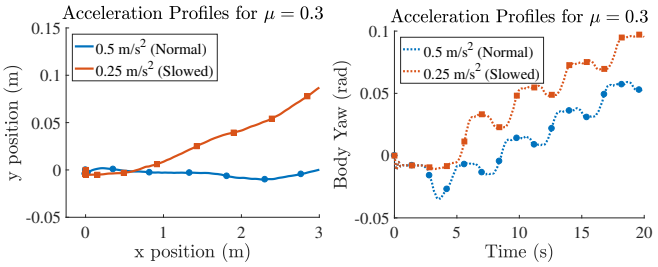

Fig. 10. Effect of fast versus slow acceleration profiles on (x, y) body position and on body yaw rotation over time.

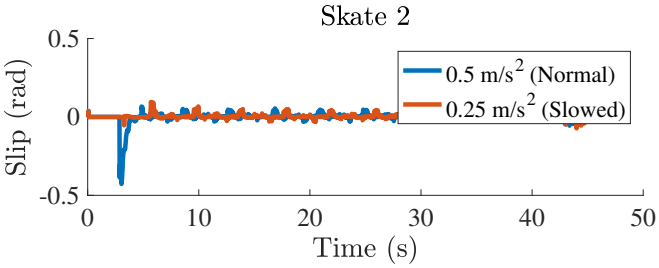

Fig. 11. Slip angle of skate 2 during trajectory execution, with peak acceleration of $0.5 m/s^2$ vs $0.25 m/s^2$.

Figures 10 and 11 compare the slower and faster acceleration cases. The (x, y) plot, at left in Fig. 10, shows the initial transient well. Slip for the faster acceleration case turns the body slightly to the right (negative yaw direction), unexpectedly canceling some of the later, steady-state rate of yaw, which was not anticipated.

Greater wheel slip in the higher-acceleration case is highlighted in Figure 11. Here, the "slip angle" is the difference between the direction of the skate motion and the direction in which the skate can roll freely with no slip. Slower acceleration removes most of the transient slip observed when initially starting the skating motion, but there is not a clear benefit in overall tracking performance.

3) Pushing off with the free limb: While push-off, analogous to skate boarding, was successful, it demonstrated no performance benefits (in speed or accuracy). See our video supplement for an example of this motion.

IV. Design for Variable Terrain Challenges

Toward more generalized motion planning, the forward-rolling motion primitives discussed in the previous section

are now augmented by including diagonal trajectories, curved paths, variable friction and mild bumps on terrain. In this section we design (and simulate with Klampt) such skating motions for both three- and four-limb skating. A short mp4-format video is provided within the supplementary materials for this paper, illustrating the motions described below, as well as others that are not described, due to space constraints.

A. 20 (m) *Straight Trajectory*

Straight trajectories were already discussed in Sections III-A and III-B, where results were presented assuming a friction coefficient of $\mu = 0.3$ between each skate and the ground. In Figure 12, we present additional results for a range of values of μ, with a steady-state velocity of 0.5 (m/s). Errors are quite small for symmetric, 4-wheel skating, in the leftmost subplots. Even for the lowest friction tested ($\mu = 0.1$), error in end state is only about 0.5 meters, or 2.5% of the total 20-meter desired distance.

For 3-limb skating, results are similar for all $\mu \geq 0.3$, with desired forward velocity and a net yaw rate of about 0.26 $^\circ/s$ (i.e., turning radius of about 110 meters). Slip is quite noticeable for $\mu = 0.1$, however, with speed reduced to about 80% of the desired rate and a tighter (unplanned) turning radius (about 40 meters) due to slip.

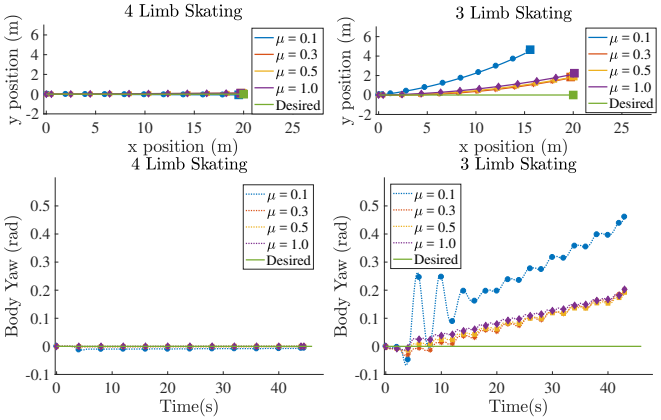

Fig. 12. Tracking a 20 (m) straight ahead trajectory with four (left) or three (right) skates over varying μ.

B. 10 (m) *Diagonal Trajectory*

Here, motions are planned to move the body along a straight line, oriented 30° to the left (nautical "port" side) with respect to the previous, forward-facing trajectories, to test omnidirectional locomotion. Relative motions of the skates (with respect to the body) are now generalized to travel perpendicular to the planned body motion, which is an effective parameterization across all tested motions. To better visualize this, refer to the lower right subplot of Figure 3: the relative motion of the skate in this example is also planned to be exactly perpendicular to the absolute body velocity at the ground contact for this skate. This rule for planning relative skate directions is used across of all examples within this paper. Rules for planning relative phase between skates and for setting skate angles remain unchanged from Sec. III-A.

Figure 13 shows results. As there is inherently less symmetry between limbs when the robot travels diagonally, there are greater tracking errors, as expected. Compared with the forward-facing trajectories (at left, in Fig. 12), four-limb skating does show more sensitivity to μ, but it is still a mild effect. Three-limb skating is significantly more sensitive to changes in μ; however, there is a relatively smooth mapping between μ and the resulting offset in yaw angle, which occurs primarily during acceleration at the start. A bifurcation in behavior occurs between friction values of 0.1 and 0.3, i.e., slip is dramatic for $\mu = 0.1$.

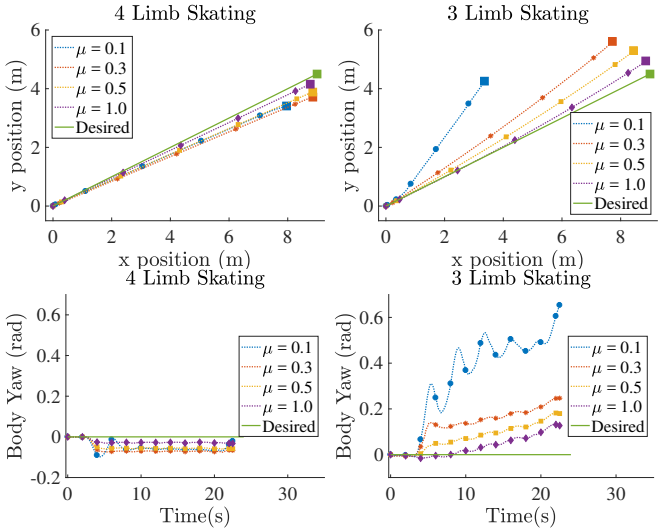

Fig. 13. Tracking a $\pi/6$ diagonal trajectory from straight ahead with four (left) or three (right) skates over varying μ.

C. 2 (m) *Radius Circle Trajectory*

To plan circular body trajectories, we again choose relative skate motions that are perpendicular to absolute velocity of the body-fixed coordinate frame at the ground contact of each skate. For curved trajectories, this means each skate oscillates back and forth exactly on the line extending radially from the desired ICR to its particular ground contact (see bottom left of Fig. 3 again).

Simulations in Klampt track a circle trajectory of radius 2 (m). For $\mu = 0.1$, three-limb skating cannot complete the trajectory, which is shown in the accompanying video. For the other coefficients of friction, three-limb skating performs quite well, and actually close to as well as 4 limb skating, unlike for the previous motions.

D. *Monte Carlo Simulations over Rough Terrain*

Over flat terrain, regardless of the coefficient of friction, four-wheel skating outperforms the accuracy of three-wheel skating, albeit sometimes only by a small margin. This is no longer the case on bumpy terrain.

We created "smooth" wavy terrains via spline fits of randomly generated heights across a 2D grid. We present results here for terrains with peak bump heights of 0.1 (m) and 0.2 (m), for the 20 (m) straight trajectory previously

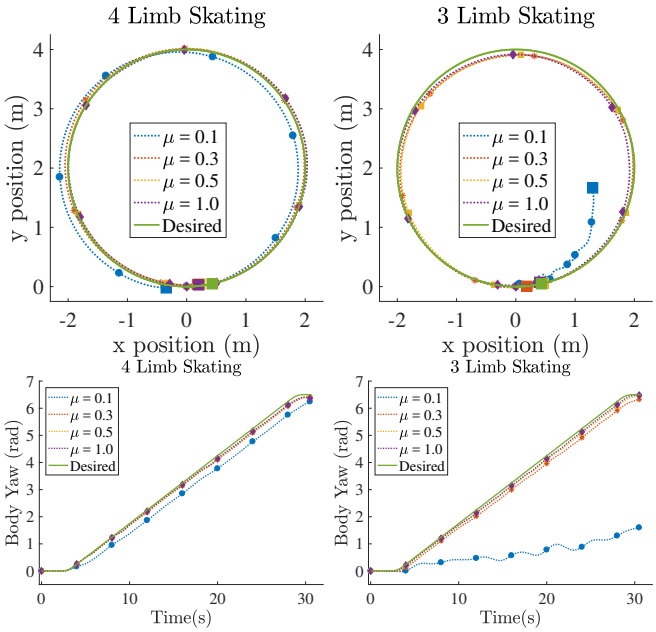

Fig. 14. Tracking a circular trajectory with radius 2 (m) with four (left) or three (right) skates over varying μ.

studied on flat terrain (in Sec. IV-A) for 20 open-loop trials with each of four values of μ, randomizing initial position and orientation on terrain for each trial.

Figures 15 and 16 show the final (x, y) coordinates of the robot for each of the trials. Over the 0.1 m maximum height rough terrain, save for the $\mu = 0.1$ case, three limb skating always travels close to the desired 20-m distance, though the body trajectory may be offset by up to 10°, due to initial yaw perturbations. This significantly outperforms four limb skating, where there is a much broader distribution of end states, corresponding to intermittent slip throughout motion and not just at during initial acceleration (as for three-skate motions).

The discrepancy between the two primitives becomes even more significant over the rougher terrain with 0.2 (m) bumps. Three-limb skating is still reliable for $\mu = 1$, with some bifurcations in behavior appearing at lower frictions. With four skates, however, behavior is unreliable regardless of the value of μ. RoboSimian consistently has trouble going up the small wavy hills and sometimes even rolls backwards, getting stuck in a trough where it often repeatedly slips and rolls/slides back down. The supplementary video shows an example of this for 4 limb skating.

V. Conclusions and Discussion

Agile wheeled locomotion is one route toward increasing energy efficiency, stability, and speed simultaneously on mild terrain for limbed robots also capable of rough terrain walking and/or dexterous manipulation tasks. In this paper, we outline design of and present performance analyses for a small family of motion primitives, exploring trade-offs between speed and accuracy as a function of (stochastic) terrain properties, toward facilitating both high-level planning

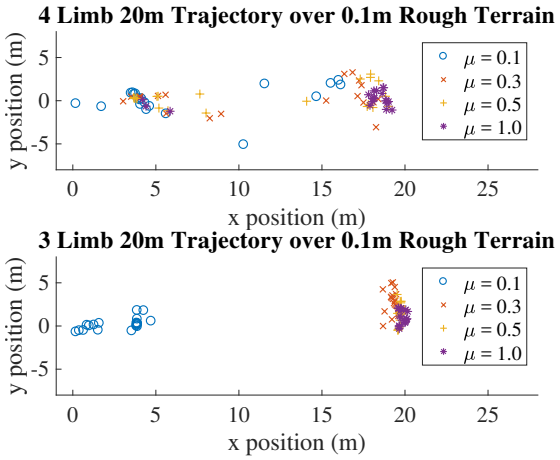

Fig. 15. Monte Carlo simulations of a 20 (m) straight trajectory over "smooth" rough terrain that varies randomly uniformly over 0.1 (m).

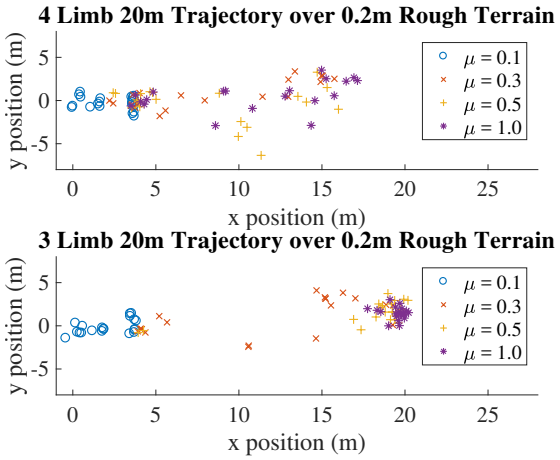

Fig. 16. Monte Carlo simulations of a 20 (m) straight trajectory over "smooth" rough terrain that varies randomly uniformly over 0.2 (m).

structures and low-level learning algorithms.

For high-level planning, we envision use of skating primitives within a larger framework, to avoid obstacles, meet desired waypoints, and reach particular end destinations on mild terrain. Real-world locomotion will involve terrain with variable contact friction and unevenness, along with inherent time delays for sensor estimates of 6-DOF body pose based on processed vision and lidar information. One practical planning strategy would therefore be to employ a sequence of well-characterized but stochastic open-loop dynamic maneuvers [19], using piece-wise composition with a receding horizon approach for replanning to cope with uncertainty [20]. Such a strategy is in the spirit of sequential composition via a funneling approach [21]; i.e., with a set of individual controllers that can be nested, with the variability in end state of one sequence easily with the basin of attraction of the next sequential controlled action.

A second purpose of this work is to explore uncertainty propagation of various skating primitives, toward selecting and parameterizing low-level motion primitives for optimization through learning algorithms. In particular, we highlight

that skating with three wheels (1) produces greater yaw disturbances and (2) results in more continuity and repeatability as parameterizations and/or noise vary. For example, Figures 8, 9 and 13 show yaw increasing smoothly as μ goes down, for $\mu > 0.1$, and Figures 15 and 16 show more repeatable traction (i.e., clustering of end skate) for three-wheel skating, while results using four wheels yield more bifurcations and fewer examples of "smooth variations" in behavior. Correspondingly, we anticipate that three-wheeled skating can be used more effectively within gradient-based learning algorithms, to deliberately exploit slip for more dynamic, unactuated and agile maneuvers.

Finally, we note that the fidelity of dynamic simulations is an open question and ongoing research challenge in itself; real robot locomotion will vary somewhat from simulation predictions. In our experience, simulations provide an important step in efficiently identifying and pre-tuning behaviors that are later verified and/or tweaked on real hardware, also enabling safe and systematic development of dynamic motions. We highlight that ensuring robustness to parameter variability within simulation, which is a central goal in this work, typically improves real-world robustness, as well.

REFERENCES

[1] B. W. Satzinger, C. Lau, M. Byl, and K. Byl, "Experimental results for dexterous quadruped locomotion planning with Robosimian," in *Proc. Inernational Symposium on Experimental Robotics (ISER 2014)*. Springer, 2016, pp. 33–46.

[2] ——, "Tractable locomotion planning for Robosimian," *The International J. of Robotics Research*, vol. 34, no. 13, pp. 1541–1558, 2015.

[3] K. Byl, M. Byl, and B. Satzinger, "Algorithmic optimization of inverse kinematics tables for high degree-of-freedom limbs," in *Proc. ASME Dynamic Systems and Control Conference (DSCC)*, 2014.

[4] P. Hebert, M. Bajracharya, J. Ma, N. Hudson, A. Aydemir, J. Reid, C. Bergh, J. Borders, M. Frost, M. Hagman, J. Leichty, P. Backes, B. Kennedy, K. Karplus, K. Byl, B. Satzinger, and K. S. J. Burdick, "Mobile manipulation and mobility as manipulation–design and algorithms of Robosimian," *Journal of Field Robotics (Special Issue on the DRC)*, vol. 32, no. 2, pp. 255–274, 2015.

[5] S. Karumanchi, K. Edelberg, I. Baldwin, J. Nash, J. Reid, C. Bergh, J. Leichty, K. Carpenter, M. Shekels, M. Gildner, D. Newill-Smith, J. Carlton, J. Koehler, T. Dobreva, M. Frost, P. Hebert, J. Borders, J. Ma, B. Douillard, P. Backes, B. Kennedy, B. Satzinger, C. Lau, K. Byl, K. Shankar, and J. Burdick, "Team Robosimian: Semi-autonomous mobile manipulation at the 2015 DARPA Robotics Challenge finals," *Journal of Field Robotics*, vol. 34, no. 2, pp. 305–332, 2017.

[6] S. Hirose and H. Takeuchi, "Study on roller-walk (basic characteristics and its control)," in *Proc. IEEE International Conference on Robotics and Automation (ICRA)*, vol. 4, 1996, pp. 3265–3270.

[7] G. Endo and S. Hirose, "Study on roller-walker (system integration and basic experiments)," in *Proc. IEEE International Conference on Robotics and Automation (ICRA)*, vol. 3, 1999, pp. 2032–2037.

[8] ——, "Study on roller-walker (multi-mode steering control and self-contained locomotion)," in *Proc. IEEE International Conference on Robotics and Automation (ICRA)*, vol. 3, 2000, pp. 2808–2814.

[9] ——, "Study on roller-walker - adaptation of characteristics of the propulsion by a leg trajectory -," in *Proc. IEEE/RSJ International Conference on Intelligent Robots and Systems (IROS)*, 2008, pp. 1532–1537.

[10] ——, "Study on roller-walker - energy efficiency of roller-walk -," in *Proc. IEEE International Conference on Robotics and Automation (ICRA)*, 2011, pp. 5050–5055.

[11] K. Inagaki and N. I. b. Azlizan, "Skating motion by a leg-wheeled robot with passive wheels," in *Proc. IEEE/ASME International Conference on Advanced Intelligent Mechatronics (AIM)*, 2013, pp. 524–529.

[12] N. Ziv, Y. Lee, and G. Ciaravella, "Inline skating motion generator with passive wheels for small size humanoid robots," in *Proc. IEEE/ASME International Conference on Advanced Intelligent Mechatronics (AIM)*, 2010, pp. 1391–1395.

[13] O. Matsumoto, S. Kajita, and K. Komoriya, "Flexible locomotion control of a self-contained biped leg-wheeled system," in *Proc. IEEE/RSJ International Conference on Intelligent Robots and Systems (IROS)*, vol. 3. IEEE, 2002, pp. 2599–2604.

[14] N. Takasugi, K. Kojima, S. Nozawa, Y. Kakiuchi, K. Okada, and M. Inaba, "Real-time skating motion control of humanoid robots for acceleration and balancing," in *Proc. IEEE/RSJ International Conference on Intelligent Robots and Systems (IROS)*. IEEE, 2016, pp. 1356–1363.

[15] C. Iverach-Brereton, J. Baltes, J. Anderson, A. Winton, and D. Carrier, "Gait design for an ice skating humanoid robot," *Robotics and Autonomous Systems*, vol. 62, no. 3, pp. 306–318, 2014.

[16] Boston Dynamics. (2017, February) Introducing handle. [Online]. Available: https://www.youtube.com/watch?v=-7xvqQeoA8c

[17] K. Hauser, "Robust contact generation for robot simulation with unstructured meshes," in *Proc. International Symposium on Robotics Research (ISRR)*. Springer, 2016, pp. 357–373.

[18] S. Kajita, F. Kanehiro, K. Kaneko, K. Fujiwara, K. Harada, K. Yokoi, and H. Hirukawa, "Biped walking pattern generation by using preview control of zero-moment point," in *IEEE International Conference on Robotics and Automation (ICRA)*, vol. 2. IEEE, 2003, pp. 1620–1626.

[19] K. Byl, A. Shkolnik, S. Prentice, N. Roy, and R. Tedrake, "Reliable dynamic motions for a stiff quadruped," in *Proc. International Symposium on Experimental Robotics (ISER 2008)*. Springer, 2009, pp. 319–328.

[20] N. E. Du Toit and J. W. Burdick, "Robot motion planning in dynamic, uncertain environments," *IEEE Transactions on Robotics*, vol. 28, no. 1, pp. 101–115, 2012.

[21] R. R. Burridge, A. A. Rizzi, and D. E. Koditschek, "Sequential composition of dynamically dexterous robot behaviors," *International Journal of Robotics Research*, vol. 18, no. 6, pp. 534–555, June 1999.